Materials Advances

ROYAL SOCIETY OF CHEMISTRY

PAPER

View Article Online
View Journal | View Issue

Cite this: *Mater. Adv.*, 2021, **2**, 1090

Durable polymeric *N*-halamine functionalized stainless steel surface for improved antibacterial and anti-biofilm activity†

Rajani Kant Rai, *[a] Hemalatha Kanniyappan,[b] Vignesh Muthuvijayan, [b] Kesavan Venkitasamy [a] and Athipettah Jayakrishnan‡*[a]

Received 23rd October 2020,
Accepted 20th December 2020

DOI: 10.1039/d0ma00828a

rsc.li/materials-advances

Bacterial adhesion and colonization on stainless steel (SSL) based surgical instruments, hospital equipment, orthopedic implants, water purification and food processing units are a major problem. Imparting rechargeable antibacterial properties to SSL offers the prospect of a reusable and clean surface. In this study, the SSL surface was functionalized with a hydantoin-based antibacterial polymer that prevents bacterial adhesion and colonization. A new hydantoin monomer with three halogen binding sites, (*Z*)-*N*-((4-(2,5-dioxoimidazolidin-4-ylidene)methyl)phenyl)methacrylamide (DMPM), was synthesized, characterized and copolymerized with a commercially available 3-(methacryloyloxy)propyltrimethoxysilane monomer to develop the antibacterial polymer. The SSL surface was treated with piranha solution and the copolymer was covalently immobilized on the surface. The modified surface was examined for its antibacterial and anti-biofilm activity. The modified surface exhibited total kill (6 log reduction) of bacteria such as *S. aureus* and *E. coli* in 10 and 12 min respectively. The anti-biofilm activity of the modified surface was evaluated using a combination of fluorescence-based metabolic activity and scanning electron microscopy imaging suggested the comprehensive damage of *S. aureus* and *E. coli* biofilm architecture.

1. Introduction

Stainless steel (SSL) is widely used in surgical instruments, in various hospital equipment, in orthopedic implants and in water purification and food processing units due to its mechanical properties and resistance to corrosion.[1–4] However, several reports suggest that the SSL surface has the ability to harbor bacterial biofilms of different genera such as *Listeria*, *Staphylococcus*, *Escherichia*, *Bacillus* and *Pseudomonas* that may lead to cross-contamination and fouling of the surface.[5,6] Therefore, controlling the adhesion and growth of bacteria on the SSL surface has great potential to prevent cross contamination and development of stable biofilms. In order to render the SSL surfaces antibacterial, various surface modification strategies such as deposition of biocidal metals like silver, copper, zinc and nickel, chemical vapor deposition, electroless nickel, layer-by-layer assembly of charged polyelectrolytes, sol gel method, *etc.* have been employed.[7–13] Surface modification of SSL with natural or synthetic polymers such as antimicrobial peptides and inorganic–organic hybrid coatings of polysilsesquioxane and quaternized poly(2-(dimethyamino)ethyl methacrylate) have been reported to inhibit bacterial colonization.[12,14] Generally, the above mentioned approaches exhibit migration of antimicrobial agents from the surfaces, and longer contact times are needed to inactivate the bacteria, which limit their practical application. In this context, functionalization of various surfaces using *N*-halamine containing polymers has emerged as a potential strategy to prepare antimicrobial surfaces due to their rapid action, broad spectrum activity, cost effectiveness and rechargeability.[15–18] The antimicrobial mechanism involves the transfer of oxidative halogen from *N*-halamine to the microbial receptors. *N*-Halamine based polymers have been mainly used in applications such as water disinfection, antimicrobial paints, antimicrobial treatment of textiles, *etc.*[15–28] There are few reports which describe the application of *N*-halamine in the development of antimicrobial SSL surfaces.[29–32] The methods usually require prolonged exposure time to completely deactivate the microbes.[29–31] To the best of our knowledge, there is only one report on the surface modification of SSL using *N*-halamine based copolymers where a 6 log reduction (total kill) of the organisms has been reported within 15 min of contact time.[32] Generally,

[a] *Chemical Biology Laboratory, Department of Biotechnology, Bhupat and Jyothi Mehta School of Biosciences, Indian Institute of Technology Madras, Chennai 600 036, Tamil Nadu, India. E-mail: rk.120988@gmail.com*
[b] *Tissue Engineering Laboratory, Department of Biotechnology, Bhupat and Jyothi Mehta School of Biosciences, Indian Institute of Technology Madras, Chennai 600 036, Tamil Nadu, India*

† Electronic supplementary information (ESI) available. See DOI: 10.1039/d0ma00828a

‡ Present address: Raja Ramanna Fellow, Rajiv Gandhi Centre for Biotechnology, Jagathy, Trivandrum 695 014, Kerala, India. E-mail: jayakrishnana@rgcb.res.in

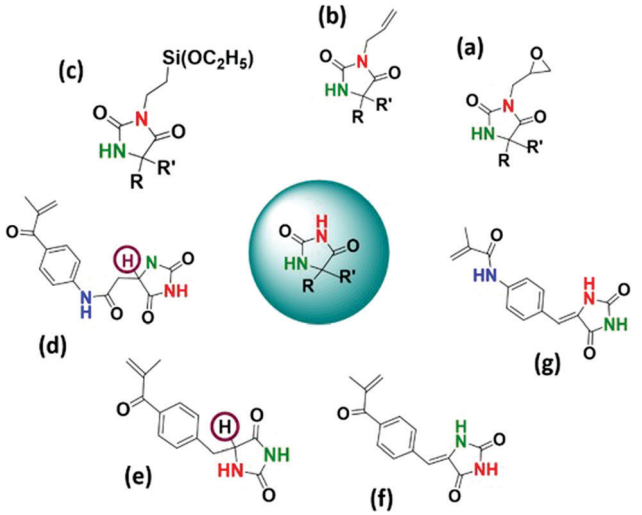

Scheme 1 Hydantoin monomers with lost imide position for Cl binding (a–c), monomers containing tertiary hydrogen that can prompt the release of HCl after chlorination (d and e), a stable monomer with 2 Cl binding sites (f) and a stable monomer with 3 Cl binding sites (g).

hydantoin (cyclic *N*-halamine) monomers are synthesized by attaching a polymerizable moiety to 5,5′-disubstituted hydantoin, thereby restricting the halogen capture to only at the amide position[17–21,33–36] (Scheme 1a–c). In our previous reports, we have shown that hydantoin monomers with more than one chloramide function could be synthesized and copolymerized without sacrificing the halogen binding site in the hydantoin ring.[37–39] Moreover, the presence of α-H (Scheme 1d and e) close to the N–Cl bond in the hydantoin moiety can lead to the elimination of HCl upon chlorination that adversely affects the bactericidal property and durability of the polymer and can cause corrosion of the surface.[38–41] To this end, a new hydantoin monomer (*Z*)-*N*-((4-(2,5-dioxoimidazolidin-4-ylidene)methyl)phenyl) methacrylamide (DMPM) (Scheme 2, step 1) with improved chlorine binding site was synthesized and copolymerized with 3-(methacryloyloxy)propyl trimethoxysilane (MPTS) using 2,2′-azobisisobutyronitrile (AIBN) as the initiator. SSL coupons pretreated with piranha solution were immobilized with acid hydrolyzed poly(DMPM-*co*-MPTS) *via* metal–oxane bond formation. The modified SSL surface generated antibacterial chloramide function on treatment with aqueous bleach. The SSL surface challenged with Gram-positive *S. aureus* and Gram-negative *E. coli* bacteria exhibited total kill (6 log reduction) within 10 and 12 min respectively. Moreover, the modified surface displayed potent anti-biofilm activity, long term rechargeability and durability and was nontoxic to a fibroblast cell line.

2. Experimental section

2.1. Materials

A medical grade 316 SSL sheet of 0.50 mm thickness obtained from Jainex Steel and Metal, Mumbai, India was cut into 2.0 cm × 2.0 cm coupons. Diisopropylethylamine (DIPEA), 4-nitrobenzaldehyde, and ammonium acetate were obtained from Spectrochem Ltd, Mumbai, India. 3-(Methacryloyloxy)propyltrimethoxysilane (MPTS), methacryloyl chloride, palladium on activated charcoal and hydantoin were obtained from Alfa Aesar, Mumbai, India. 4-Dimethylamino pyridine (DMAP), AIBN, *N*,*N*-dimethyl formamide (DMF), barium oxide, sodium hypochlorite, silica gel (100–200 mesh) and hexane were obtained from Sigma Aldrich or HiMedia Labs, Mumbai, India. All other reagents and chemicals were of analytical grade. Milli Q water was employed throughout. MPTS was washed with aqueous sodium hydroxide followed by water to remove the inhibitors, dried over anhydrous sodium sulfate and distilled

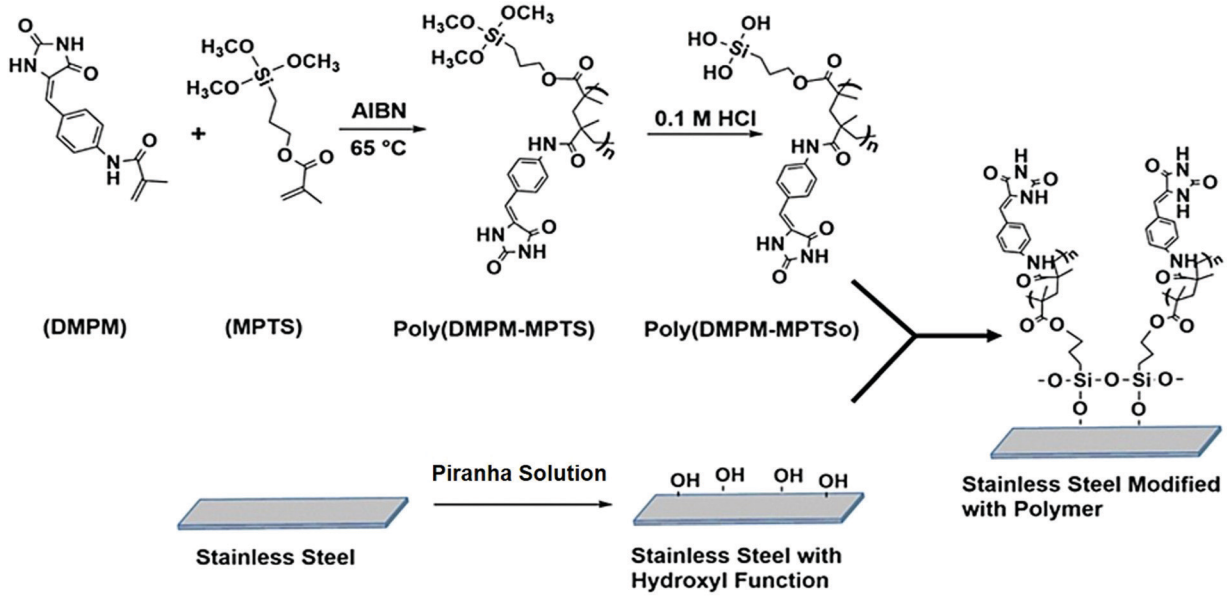

Scheme 2 Synthesis of the hydantion based polymer and functionalization on the SSL surface.

under reduced pressure before use. Dry DMF was prepared by drying the solvent overnight over barium oxide followed by vacuum distillation.

2.2. Characterization

Nuclear magnetic resonance (NMR) spectra were recorded on an AVANCE III 500 MHz spectrophotometer (Bruker, Germany) with DMSO-d_6 as the solvent. Fourier transform infrared (FTIR) spectra were recorded using a PerkinElmer Spectrum1 FT-IR instrument using KBr pellets. Thermogravimetric analysis (TGA) and differential scanning calorimetry (DSC) were carried out using PerkinElmer (TGA7, Q500 Hi-Res TGA) and PerkinElmer (DSC7, Q200 MDSC) instruments respectively, at a heating rate of 10 °C min^{-1} under a nitrogen atmosphere. X-ray photoelectron spectroscopy (XPS) was done on a Ulvac-Phi Quantes (Japan) instrument with Mg Kα radiation. The elemental composition of the polymers was determined using a CHNS/O PerkinElmer 2400 series analyser. An ELISA microplate reader (Spectrum Max 5; Molecular Devices, USA) was employed to evaluate cell viability. Gel permeation chromatography (GPC) was used to determine the weight average molar mass of the copolymer in a Shimadzu (Japan) instrument. THF was used as the mobile phase at a flow rate of 1 mL min^{-1} with an R401 refractive index detector and a 7725 Rheodyne injector. Polystyrenes of known MW (Jordi Labs, USA) were used as the standards. The 3-D surface topography of the unmodified (Control) and modified surface was visualized using AFM (Park System, XE-100 AFM) in tapping mode. Images are shown for an area of 10 μm × 10 μm.

2.3. Synthesis of the hydantoin monomer

To synthesize the hydantoin monomer, initially 4-nitrobenzaldehyde (5 g, 33.1 mmol), ammonium acetate (5.1 g, 66.2 mmol) and hydantoin (5.1 g, 51 mmol) were dissolved in 80 ml of glacial acetic acid. The reaction mixture was refluxed for 20 h and the resulting precipitate was filtered, washed with water followed by ethanol and dried under vacuum to obtain (*Z*)-5-(4-nitrobenzylidene)imidazoline-2,4-dione (NBID). Further, NBID (3 g, 12.86 mmol) was dissolved in a mixture of anhydrous THF (30 ml) and DMF (50 ml), followed by addition of 300 mg of 10% palladium on activated charcoal (Pd/C) as a catalyst. The reaction mixture was stirred for 20 h under a hydrogen atmosphere to obtain (*Z*)-5-(4-aminobenzylidene)imidazoline-2,4-dione (ABID). Finally, ABID (2 g, 7.37 mmol) was dissolved in anhydrous DMF under a nitrogen atmosphere, DIPEA (1.92 ml, 11.06 mmol) and a catalytic amount of DMAP were added followed by drop-wise addition of methacryloyl chloride (0.87 ml, 8.84 mmol) at 0 °C. The reaction mixture was magnetically stirred for 4 h at room temperature to complete the reaction. The mixture was diluted with ethyl acetate and washed with aqueous $NaHCO_3$ followed by water, dried over anhydrous Na_2SO_4 and distilled under vacuum to remove the solvent. The obtained residue was purified through column chromatography on silica gel to yield DMPM.

2.4. Synthesis of the copolymer and surface modification of SSL

A 25 ml pressure tube was charged with different concentrations of DMPM, MPTS and 0.1% AIBN in dry THF (10 ml) and purged with N_2 for 30 min. The polymerization was allowed to proceed at 60 °C in an oil bath for 24 h. The resulting polymer was precipitated in methanol and dried under vacuum to obtain a hydantoin based polymer, poly(DMPM-*co*-MPTS). The SSL coupons were treated with acetone, ethanol and water for 10 min in each solvent. After drying, the coupons were treated with piranha solution (H_2O_2/H_2SO_4 in 7 : 3 volumetric ratio) for 30 min and then dried in an air oven.[42] The coupons were then immersed in 20 ml of acetone/methanol (1 : 1) containing 1.5 g of poly(DMPM-*co*-MPTS) for 1 h to obtain uniform adsorption of the polymer on the surface.[43]

The adsorbed polymer was hydrolyzed with 0.1 M HCl to convert the Si–OCH_3 group to Si–OH. Finally, the coupons were washed with ethanol and water and dried in a N_2 atmosphere and cured at 90 °C for 1.5 h to promote metal–oxane bond formation between SSL surface and coated polymer (Scheme 2, step 2).

2.5. Chlorination and determination of oxidative chlorine content

500 mg of finely powdered hydantoin containing copolymer poly(DMPM-*co*-MPTS) was treated with 9–12% sodium hypochlorite solution at pH 7 (adjusted by 6 N HCl) for 1.5 h. After chlorination, the polymer was washed thoroughly with water and dried at 45 °C for 1 h to remove free chlorine.[37] The oxidative chlorine content of the polymer was determined by the standard iodometric/thiosulfate titration method.[39] Blank titration was performed under similar conditions as control. The percentage chlorine content was calculated using the following equation:

$$\text{Percentage chlorine} = \frac{35.5 \times (V_{Cl} - V_O) \times 10^{-3} \times 0.01}{2 \times W_g} \times 100$$

where V_{Cl} and V_O are the volumes (mL) of the sodium thiosulfate solution consumed in the titration of the copolymer solution and the blank, respectively, and W_g is the weight of the polymer. Each test was repeated three times and the average was taken.

2.6. Antibacterial efficacy testing

The bactericidal activity of the SSL surface modified with the hydantoin based polymer was evaluated against representative Gram-positive *S. aureus* (ATCC 29213) and Gram-negative *E. coli* (BL21) bacteria. Initially, the target bacterial strains were allowed to grow in nutrient broth overnight at 37 °C in a rotatory shaker at 180 rpm. The bacterial cultures were harvested and washed with phosphate buffered saline (PBS, pH 7.4). A ''sandwich method'' was adopted to evaluate the antibacterial efficacy of the modified SSL surface. A surface modified SSL coupon was exposed to 30 μL of bacterial suspension containing 6–6.5 log_{10} CFU mL^{-1}, and a second surface modified SSL coupon was placed on the top of the first with a sterile beaker on top to ensure good contact of bacteria with the surface. After a predetermined contact time the coupons were immersed in 5 mL of 0.03 wt% sterilized aqueous sodium thiosulfate solution to quench the active chlorine and thus terminate the disinfection activity.[39] The quenched samples were vortexed, serially diluted and 100 μL of each dilution was placed on a nutrient agar plate.

The plates were incubated at 37 °C for 24 h to grow the colony. The unchlorinated surface was taken as a negative control. The percentage reduction was calculated using the following formula:

$$\text{Percentage reduction} = \frac{X - Y}{X} \times 100$$

where X is the population of CFU on the control plate and Y is the population of CFU on the test plate.

The log reduction was then calculated as

$$\text{log reduction} = \log(X - Y)$$

The plate counting experiments were performed in triplicate using fresh bacterial inocula and statistical analysis was performed using Microsoft Excel 2013.

2.7. Biofilm growth inhibition assay

The anti-biofilm activity of the SSL surface modified with the hydantoin based copolymer was determined using metabolic activity based colorimetric assay.[44] Initially, the SSL coupon was placed in a 24 well plate and 200 μL of bacterial culture containing *S. aureus* or *E. coli* supplemented with 0.4% of glucose was spread on the coupon surface. The plate was then incubated under dark and humid conditions for 24 h at 37 °C to allow biofilm growth. Further, the coupon was removed from the well and gently washed with sterile PBS to remove non-adhered planktonic cells. The washed coupon was transferred into a fresh 24 well plate with the addition of 1 mL of nutrient broth containing 50 μM resazurin sodium salt to quantify the metabolic activity of the biofilm formed on the surface. The fluorescence intensity of the solution was measured at room temperature using an excitation filter at 530 nm and an emission filter at 580 nm in a fluorescence reader.

SEM based imaging of *E. coli* and *S. aureus* was also employed to determine the potential of SSL surfaces for inhibition of biofilm growth.[45] 200 μL of targeted bacterial suspension supplemented with 0.4% of glucose was spread on a SSL coupon modified with the chlorinated polymer. Further, the coupon was incubated under dark conditions at 37 °C for 24 h to grow the biofilm. The coupon was removed from the well plate, gently washed with water, fixed with 2.5% glutaraldehyde followed by drying in a sterile environment, sputtered with gold and imaged using SEM. The same procedure was applied for the pristine SSL surface or the SSL surface modified with the unchlorinated polymer that served as the control.

2.8. Durability and regenerability testing

Recharge and discharge cycles were performed to evaluate the durability and regenerability of SSL coupons modified with the chlorinated hydantoin polymer as reported before.[46] Immersion of chlorinated coupons to quench the active chlorine in 0.03% of aqueous sodium thiosulfate solution is termed as ''discharge''. Further, the coupons were washed and treated with 9–12% of sodium hypochlorite solution to load the polymer with active chlorine which is termed as ''recharge''. The chlorine content and bactericidal activity were determined after 5, 15, 25 and 45 cycles to determine the durability and regenerability of the modified SSL surface.

2.9. *In vitro* cytotoxicity assay

The cytotoxicity assays were performed using the MTT based colorimetric method.[47] The NIH/3T3 cells were initially propagated in a 25 ml tissue culture flask containing DMEM supplemented 10% FBS. Subsequently, the cells were seeded in 48-well plates (1.0×10^4 cells per well) and incubated in 5% CO_2 at 37 °C for 24 h. The medium was replaced with fresh 10% FBS-containing DMEM, followed by the placing of polymer coated with chlorinated or unchlorinated SSL surface. After 48 h, MTT solution (5 mg mL^{-1}) was added and the plates were incubated for 4 h at 37 °C. The supernatant was gently removed and the formazan crystals were solubilized in DMSO and the optical density was read at 570 nm in a mutiplate reader.

For fluorescence-based imaging, NIH/3T3 cells were seeded in a 48-well plate and incubated at 37 °C for 24 h. Further, the medium was replaced with fresh 10% FBS-containing DMEM, followed by the introduction of polymer coated with chlorinated or unchlorinated SSL surface. After 48 h, the modified SSL coupon was removed, the medium was aspirated and cells were washed 4 times with PBS to remove dead cells. To determine cell viability and nuclear integrity, FDA and DAPI staining methods were employed.[48] Stained cells were excited at 488 nm (FDA) and 360 nm (DAPI) to visualize and image under a fluorescence microscope.

2.10. Statistical analysis

Statistical analyses were performed using Prism (v5.0, GraphPad Software, USA). The data were assessed with ordinary one-way ANOVA followed by a Tukey *post hoc* test. A value of $p < 0.005$ was considered as significant.

3. Results and discussion

3.1. Synthesis of the hydantoin monomer

Initially, (*Z*)-5-(4-nitrobenzylidene)imidazoline-2,4-dione (NBID) was synthesized and characterized by NMR (^{1}H and ^{13}C) and FTIR. Tethering of the hydantoin moiety to 4-nitrobenzaldehyde was confirmed by amide and imide proton signals at δ 11.41 ppm and 10.89 ppm for the hydantoin ring in the ^{1}H NMR spectrum (Fig. S1, ESI†). In addition, the ^{13}C NMR spectrum showed the presence of amide and imide carbonyl carbon signals at δ 165.70 ppm and 156.23 ppm respectively (Fig. S2, ESI†). In the FTIR spectrum, the peaks at 3225 cm^{-1} and 1748 cm^{-1} were attributed to NH and C=O respectively confirming the synthesis of NBID (Fig. S3a, ESI†).

Further, the appearance of two characteristic bands for primary amine around 3230 cm^{-1} confirmed the reduction of the nitro group to amine suggesting the formation of ABID (Fig. S3b, ESI†). The introduction of the singlet peak at δ 4.89 ppm for the amine group in the ^{1}H NMR spectrum also confirms the synthesis of the compound (Fig. S4, ESI†). Finally, the polymerizable moiety was

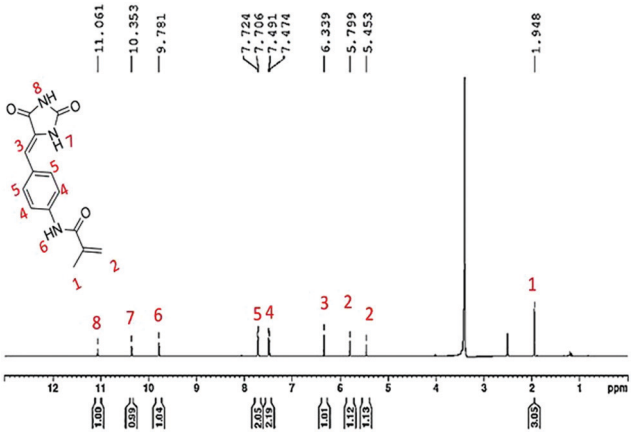

Fig. 1 ^{1}H NMR of the hydantoin monomer (DMPM).

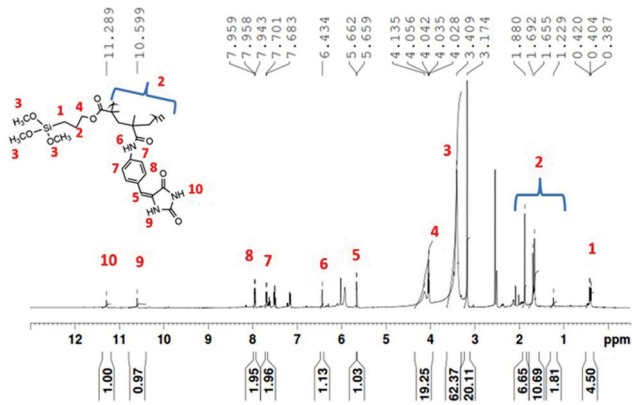

Fig. 3 ^{1}H NMR of the hydantoin based copolymer (DMPM-*co*-MPTS).

tethered by amide bond formation with the methacryloyl chloride to give rise to the hydantoin monomer. In the ^{1}H NMR spectrum, the arrival of peaks at δ 6.33 ppm, 5.79 ppm and 1.94 ppm for olefinic protons and $-CH_3$ respectively suggested the attachment of the polymerizable moiety (Fig. 1). In addition, the appearance of peaks at δ 167.30 ppm, 140.71 ppm, 114.50 ppm and 19.12 ppm for C═O, ═C–, ═CH_2 and CH_3 respectively in the ^{13}C NMR spectrum reflected the formation of the hydantoin monomer (Fig. S6, ESI†). Further the presence of a peak at 1640 cm^{-1} for –C═C stretching in the FTIR spectrum suggested the formation of the hydantoin monomer (Fig. 2a).

3.2. Synthesis of the copolymer and surface modification of SSL

The copolymerization of hydantoin monomer DMPM with MPTS was carried out *via* free radical polymerization. The resulting copolymer was characterized by GPC, FTIR, NMR, and XPS. The weight average molecular weight (M_w) and number average molecular weight (M_n) of the polymers containing 10 mol% of hydantoin monomer were 13 500 Da and 5300 Da respectively with a polydispersity index of 2.54 (Fig. S7, ESI†). The FTIR spectrum of the hydantoin monomer (DMPM) showed the characteristic peaks of –NH, CO, –CC and corrugated peaks for the aromatic ring at 2980 cm^{-1}, 1750 cm^{-1}, 1640 cm^{-1} and 698 cm^{-1} respectively (Fig. 2a). The spectrum of the pristine polymer (PMPTS) showed the peaks for –CH, C═O and Si–OCH_3 at 3200 cm^{-1}, 1750 cm^{-1} and 1200 cm^{-1} respectively (Fig. 2b). In the copolymer poly(DMPM-*co*-MPTS), the disappearance of stretching vibration of –C═C suggested the introduction of the hydantoin monomer in the copolymer. Other characteristic peaks of the hydantoin monomer were merged in the polymer peak (Fig. 2c). In the ^{1}H NMR spectrum, the appearance of signals at δ 11.28 ppm and 10.59 ppm confirmed the incorporation of the hydantoin monomer in the polymer (Fig. 3).

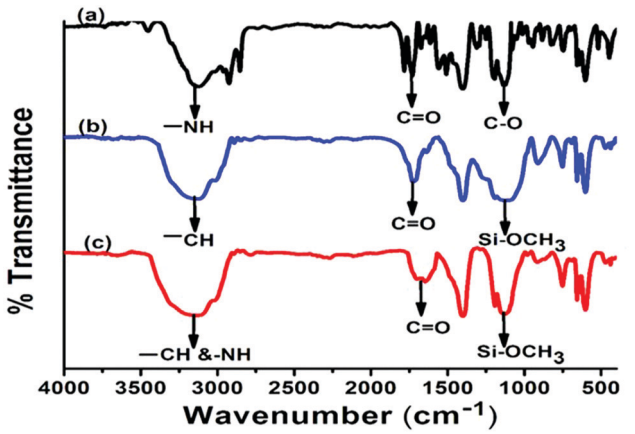

Fig. 2 FTIR spectrum of DMPM (a), poly(MPTS) (b) and poly(DMPM-*co*-MPTS) (c).

Moreover, the disappearance of olefinic protons from the hydantoin monomer (DMPM) and commercial monomer (MPTS) in the NMR spectrum suggested the formation of the copolymer *via* free radical polymerization. It should be pointed out that we have not determined the copolymer composition in poly (MDMPM-*co*-MPTS) since the reactivity of these two monomers may be different.

In addition, XPS analysis was performed to understand the surface chemistry of the polymer (Fig. 4a). The XPS spectrum of poly(DMPM-*co*-MPTS) exhibited an additional peak for N 1s at 400 eV along with C 1s and O 1s at 400 eV and 285 eV respectively suggesting the incorporation of the hydantoin monomer in the copolymer. Further, the deconvolution of the C 1s peak revealed the peak division for C–N along with C–C, C–O and C═O again suggesting the incorporation of the hydantoin monomer in the copolymer. Signal processing of N 1s revealed the peak division for amide and imide nitrogen. Peaks assigned to the photoelectrons from Si 2s and Si 2p at 154 and 101 eV from the base polymer confirmed the siloxane moiety. The synthesized polymer was employed for surface modification of SSL. The surface was characterized using XPS (Fig. 4b). The SSL surface treated with the piranha solution exhibited the intense peak of O 1s (43.8%) at 532 eV attributed to surface oxidation treatment (Fig. 4b(i)) as compared to (35. 9%) for the C 1s peak. Further, the SSL surface modified with the polymer exhibited the N 1s, Si 2s and Si 2p peaks at 400, 154 and 101 eV respectively along with C 1s and O 1s confirming the coating of the polymer over the surface (Fig. 4b(ii)). In this, oxygen (O 1s at 532 eV, 36.4%),

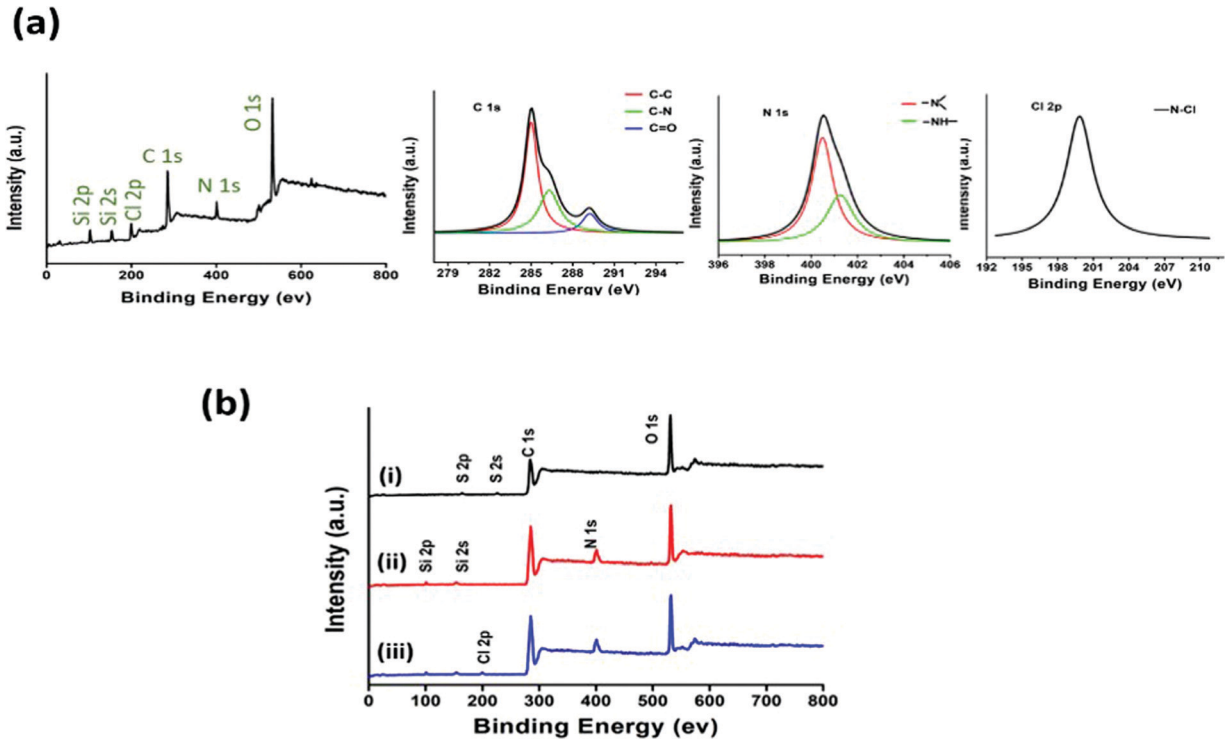

Fig. 4 XPS analysis of poly(DMPM-*co*-MPTS) (a) and modified SSL surfaces (b). Piranha treated SSL surfaces (i), SSL surfaces modified with the polymer (ii) and SSL surfaces modified with the chlorinated polymer (iii).

carbon (C 1s at 285 eV, 57.4%), nitrogen (N 1s at 400 eV, 2%) and silicon (Si 2s and 2p at 101 and 154 eV, 4.2%) were obtained.

The modified SSL surface upon chlorination exhibited the Cl 2p (1.52%) peak at 200 eV along with C 1s (57.2%), O 1s (36.2%), N 1s (2.1%), and silicon (Si 2s and Si 2p, 3.0%) peaks suggesting the chlorination of the hydantoin moiety (Fig. 4b(iii)). Further, the surface topography of control and modified stainless steel was visualized in tapping mode using atomic force microscopy (Fig. S9, ESI†). The control surface exhibited a surface roughness of 4.5 nm, whereas the surface after functionalization with the hydantoin based polymer showed a surface roughness of 6.4 nm. The increase in roughness is possibly due to the formation of small patches at a few places. Most of the coated surface exhibited a uniform distribution of the polymer that may provide active bactericidal activity across the surface.

3.3. Elemental analysis

Carbon, hydrogen and nitrogen contents of the polymer were quantified using a CHNOS analyzer in CHN mode. The iodometric titration method was employed to quantify the oxidative chlorine content in the chlorinated polymer. Expected enhancement of active chlorine and nitrogen content was observed upon increasing the feed ratio of the hydantoin monomer in the copolymerization reaction (Table S1, ESI†).

3.4. Thermal analysis

The thermal stability of the pristine polymer and the copolymer was analyzed using thermogravimetry (TGA) and differential scanning calorimetry (DSC). The TGA exhibited a similar degradation pattern for both the polymers (Fig. S7a, ESI†). The thermograms of both the polymers showed 10% degradation around 340 °C, whereas more than 50% degradation was observed around 500 °C and only 30% of the polymer was left at 900 °C. The observed weight loss in the polymers can be attributed to the condensation and combustion of the organic groups. From these results, it was concluded that there was no additional thermal instability observed due to the hydantoin monomer. The DSC of the pristine polymer and its corresponding copolymer is shown in Fig. S7b (ESI†). The glass transition temperature (T_g) of the copolymer modified with the hydantoin monomer was found to be 115 °C. The T_g of the copolymer was similar to that of the pristine polymer suggesting that the introduction of the hydantoin monomer did not create thermal instability in the copolymer.

3.5. Antibacterial assay

The antibacterial activity of the modified SSL surface was evaluated through the plate counting method. This study was performed with fresh inocula (varying between 6 and 6.5 $\log_{10}$ CFU mL^{-1} for both the strains) for each experiment in triplicate. The pristine SSL was treated as the control and compared to the modified and chlorinated surface for both *S. aureus* and *E. coli*. The surface modified with the chlorinated hydantoin polymer exhibited a time dependent decrease in bacterial population attributed to its exceptional antibacterial activity against both the strains (Fig. 5a and b). The surface modified with the copolymer containing 10 mol% of hydantoin monomer exhibited

improved bactericidal activity than the surface modified with 5 mol% of hydantoin monomer. The copolymer with 10 mol% of hydantoin monomer showed 2.1 log reduction and 4.6 log reduction in 5 min and 8 min respectively. While total kill was observed in 10 min of exposure to *S. aureus*, in the case of *E. coli*, total kill was observed in 12 min of exposure due to the presence of a characteristic extracellular polysaccharide layer. However, the copolymer with 5 mol% of hydantoin monomer required 15 min to exhibit the total kill against both the strains. The antibacterial study of the hydantoin polymer suggested that an increase in Cl binding sites or chlorine content in the polymer improved the biocidal property. Further, the optical micrograph images were taken for the pristine SSL (control) and surface modified with the copolymer containing 10 mol% of hydantoin monomer. The control surfaces exhibited a dense growth of bacterial cells for both the strains. However, the surfaces modified with 10% hydantoin monomer exhibited a time dependent decrease in the colony formation on the plates (Fig. 5c and d).

In order to examine whether a higher hydantoin monomer content in the copolymer would give rise to better bactericidal properties in the copolymer, we raised the hydantoin monomer content to 15 mol%. The oxidative chlorine content of the copolymer containing 15 mol% of hydantoin monomer was found to be 1.68% compared to 1.50% for the copolymer containing 10 mol% of hydantoin monomer. We performed the antibacterial assessment with the copolymer containing 15 mol% of hydantoin monomer and could not observe any significant difference as compared to the polymer containing 10 mol% of hydantoin monomer (Fig. S10, ESI†). Moreover, on increasing the monomer content to 15 mol% in the feed, the copolymer was found to lose its physical strength and was not suitable for multiple antibacterial tests in the durability and rechargeability assay.

3.6. Anti-biofilm assay

Biofilm growth on the pristine or modified SSL surface was quantified by measuring the metabolic activity using resazurin based colorimetric assay (Fig. 6a). The SSL surface modified with the unchlorinated polymer containing 10 mol% of hydantoin monomer exhibited similar metabolic activity to the control (pristine SSL surface). The surface modified with the chlorinated hydantoin polymer showed significant reduction in the metabolic activity and hence biofilm growth. Moreover, the biofilm growth inhibition increased with the increase in the hydantoin monomer ratio in the copolymer.

The surface modified with the chlorinated copolymer containing 5 or 10 mol% of hydantoin monomer exhibited 12% (*S. aureus*) and 15% (*E. coli*) or 5% (*S. aureus*) and 7% (*E. coli*) of biofilm growth respectively.

The surface modified with the chlorinated copolymer containing 5 or 10 mol% of hydantoin monomer exhibited 12% (*S. aureus*) and 15% (*E. coli*) or 5% (*S. aureus*) and 7% (*E. coli*) of biofilm growth respectively. SEM based image analysis undertaken to complement the metabolic activity measurements also suggested that the surface modified with the chlorinated polymer exhibited comprehensive damage in the biofilm growth (Fig. 6b and c). The surface modified

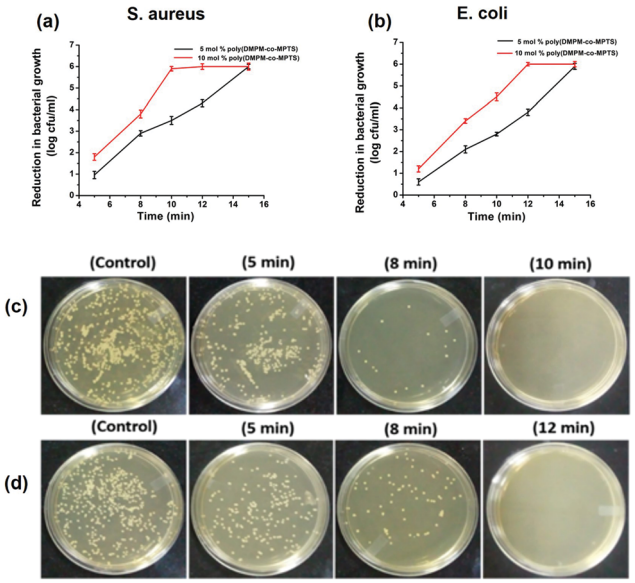

Fig. 5 Antibacterial activity of SSL modified with the chlorinated polymer. 5 mol% (a) and 10 mol% (b) of hydantoin monomer containing polymer and optical microphotographs showing the bacterial culture plates of *S. aureus* (c) and *E. coli* (d) at different times of exposure against the chlorinated polymer containing 10 mol% of hydantoin monomer.

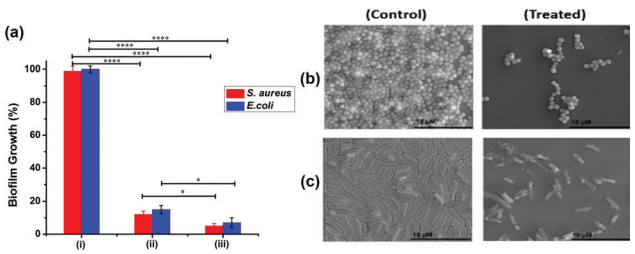

Fig. 6 Anti-biofilm activity of SSL surfaces modified with the unchlorinated or chlorinated polymer. (a) Fluorescence based measurement of biofilm growth of *S. aureus* and *E. coli* treated against the unchlorinated polymer (i) and the chlorinated polymer containing 5 mol% (ii) and 10 mol% (iii) of hydantoin monomer. (b) SEM analysis of *S. aureus* biofilm (c) and *E. coli* biofilm (d) grown on the SSL surface modified with the unchlorinated and chlorinated polymer.

with the unchlorinated polymer displayed compact protrusions and surface corrugations typically associated with mature biofilm architecture. On the other hand, the surface modified with the chlorinated hydantoin polymer showed disaggregated biofilm growth.

3.7. Durability and regenerability

The durability and regenerability were determined by estimating the oxidative chlorine content and the antibacterial activity of the surface modified with the copolymer containing 10 mol% hydantoin monomer. The modified surface was stable for 45 discharge–recharge cycles, and was able to retain 70% chlorine content. The 30% loss of chlorine binding ability (structural integrity) could be due to repetitive exposure of the polymer to

Table 1 Durability and regenerability of poly(DMPM-*co*-MPTS)

No. of washes	Antibacterial evaluation	Exposure time (min)	Chlorine content (%)
0	No colony formation	12	1.50
5	No colony formation	12	1.43
15	No colony formation	15	1.35
25	No colony formation	15	1.26
35	No colony formation	15	1.14
45	No Colony formation	18	1.04

the harsh bleaching condition (Table 1). The surface remains active for 3 cycles of antibacterial testing after each charge. After 3 cycles, the surface starts losing its activity and after 5 cycles, it does not show any activity.

3.8. *In vitro* cytotoxicity assay

Materials with applicability in clinical setting, water purification systems and food processing and storage units need to go through the evaluation for biocompatibility. To this end, the modified surface was tested for cytotoxicity on NIH/3T3 fibroblast cells using an MTT based assay. In comparison with the control (tissue culture plate), the SSL surface modified with the unchlorinated or chlorinated copolymer containing 10 mol% of hydantoin monomer exhibited negligible cytotoxicity against the fibroblast cell line (Fig. 7a). However, when the surface was modified with the chlorinated copolymer containing 15 mol% hydantoin monomer it exhibited about 20% cytotoxicity possibly due to higher chlorine content. In support of MTT based cytotoxicity assay, fluorescence microscopic analysis of cells treated with the modified surface was also carried out. Cells treated with the unchlorinated or chlorinated copolymer containing 10 mol% of hydantoin monomer showed a large number of FDA and DAPI stained cells as control, indicating the comparable viable cells in treated and control. On the other hand, cells treated with the surface modified with the chlorinated copolymer containing 15 mol% of hydantoin monomer showed fewer FDA or DAPI stained cells (viable cells), indicating the slight cytotoxic nature of the copolymer. MTT assay and fluorescence analysis indicated the nontoxic nature of the surface modified with the copolymer containing 10 mol% of hydantoin monomer suggesting potential application in biomedical and food processing industries.

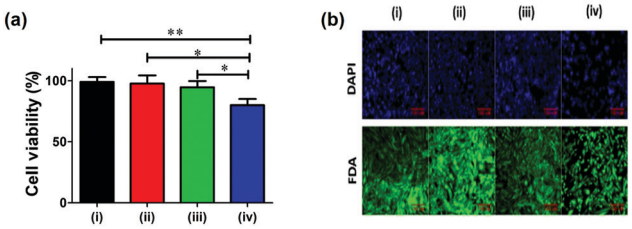

Fig. 7 Cytotoxicity assay of the SSL surface modified with the unchlorinated and chlorinated polymer. (a) MTT based cytotoxicity assay of the unchlorinated polymer containing 10 mol% (i) and 15 mol% (ii) and the chlorinated polymer containing 10 mol% (iii) and 15 mol% (iv) of hydantoin monomer; (b) fluorescence based cytotoxicity assay of the unchlorinated polymer containing 10 mol% (i) and 15 mol% (ii), and the chlorinated polymer containing 10 mol% (iii) and 15 mol% of hydantoin monomer (iv).

4. Conclusion

In this study, a new hydantoin monomer containing three Cl binding sites was synthesized and copolymerized with the commercially available siloxane based monomer, MPTS. The synthesized copolymer was covalently functionalized onto the SSL surface *via* the metal oxane bond to provide a antibacterial and anti-biofilm coating. The surface functionalized with the copolymer containing 10 mol% of hydantoin monomer exhibited total kill in 10 min against *S. aureus* and 12 min against *E. coli*. Fluorescence based metabolic activity along with SEM imaging revealed the excellent anti-biofilm activity of the SSL surface modified with the hydantoin based copolymer. Lack of tertiary hydrogen in the hydantoin ring mitigated the possible release of HCl and improved the rechargeability and durability of the coating even up to 45 discharge–recharge cycles. The coating was found to be biocompatible when tested against a fibroblast cell line. The excellent antibacterial and anti-biofilm activity, long-term rechargeability and biocompatibility of the modified SSL surface makes it a good candidate material for use in food processing and other biomedical and health-care applications where prevention of bacterial adhesion and biofilm formation is highly desirable.

Conflicts of interest

The authors declare no conflict of interests.

Acknowledgements

The authors are grateful to the Sophisticated Analytical Instrument Facility (SAIF), IIT Madras, for NMR and FTIR analysis. Thanks are due to the Department of Physics, IIT Madras, for thermal analysis of the polymer and Prof. D. Sakthi Kumar, Toyo University, Japan for assistance with the XPS analysis. RKR thanks the Department of Biotechnology, IIT Madras, for a research fellowship.

Notes and references

1 A. Bekmurzayeva, W. Duncanson, H. Azevedo and D. Kanayeva, *Mater. Sci. Eng., C*, 2018, **93**, 1073–1089.
2 C. Martins, J. Moreira and J. Martins, *Eng. Failure Anal.*, 2014, **39**, 65–71.
3 C. Smith, *Anti-Corros. Methods Mater.*, 1984, **31**, 7–9.
4 U. Thomann and P. Uggowitzer, *Wear*, 2000, **239**, 48–58.
5 L. Boulané-Petermann, *Biofouling*, 1996, **10**, 275–300.
6 A. Cherif-Antar, B. Moussa-Boudjemâa, N. Didouh, K. Medjahdi, B. Mayo and A. Flórez, *Dairy Sci. Technol.*, 2015, **96**, 27–38.
7 Y. Liu, Z. Zheng, J. Zara, C. Hsu, D. Soofer, K. Lee, R. Siu, L. Miller, X. Zhang, D. Carpenter, C. Wang, K. Ting and C. Soo, *Biomaterials*, 2012, **33**, 8745–8756.

8 X. Zhang, X. Huang, Y. Ma, N. Lin, A. Fan and B. Tang, *Appl. Surf. Sci.*, 2012, **258**, 10058–10063.
9 S. Sutha, G. Karunakaran and V. Rajendran, *Ceram. Int.*, 2013, **39**, 5205–5212.
10 K. Huang, J. Chen, S. Nugen and J. Goddard, *ACS Appl. Mater. Interfaces*, 2016, **8**, 15926–15936.
11 C. Yu, W. Ho, J. Lin, H. Yip and P. K. Wong, *Environ. Sci. Technol.*, 2003, **37**, 2296–2301.
12 P. Cao, C. Yuan, J. Xiao, X. He and X. Bai, *Surf. Interface Anal.*, 2018, **50**, 516–521.
13 A. Charlot, V. Sciannaméa, S. Lenoir, E. Faure, R. Jérôme, C. Jérôme, C. Van De Weerdt, J. Martial, C. Archambeau, N. Willet, D. Anne-Sophie, F. Charles-Andre and D. Chritophe, *J. Mater. Chem.*, 2009, **19**, 4117.
14 S. Yuan, S. Pehkonen, Y. Ting, K. Neoh and E. Kang, *Langmuir*, 2010, **26**, 6728–6736.
15 X. Sun, Z. Cao, N. Porteous and Y. Sun, *Acta Biomater.*, 2012, **8**, 1498–1506.
16 Y. Sun and G. Sun, *J. Appl. Polym. Sci.*, 2001, **80**, 2460–2467.
17 M. Chylińska, M. Ziegler-Borowska, H. Kaczmarek, A. Burkowska, M. Walczak and P. Kosobucki, *e-Polym.*, 2014, 14.
18 J. Liang, Y. Chen, X. Ren, R. Wu, K. Barnes, S. Worley, R. Broughton, U. Cho, H. Kocer and T. Huang, *Ind. Eng. Chem. Res.*, 2007, **46**, 6425–6429.
19 I. Cerkez, H. Kocer, S. Worley, R. Broughton and T. Huang, *Cellulose*, 2012, **19**, 959–966.
20 J. Kang, J. Han, Y. Gao, T. Gao, S. Lan, L. Xiao, Y. Zhang, G. Gao, H. Chokto and A. Dong, *ACS Appl. Mater. Interfaces*, 2015, **7**, 17516–17526.
21 Z. Ma, M. Yin, M. Zhang, Z. Qi, X. Ren and T. Huang, *Fibers Polym.*, 2019, **20**, 244–249.
22 C. Zhu, D. Chang, X. Wang, D. Chai, L. Chen, A. Dong and G. Gao, *Polym. Adv. Technol.*, 2019, **30**, 1386–1393.
23 S. Farah, O. Aviv, N. Laout, S. Ratner and A. Domb, *J. Controlled Release*, 2015, **216**, 18–29.
24 Y. Sun and G. Sun, *J. Appl. Polym. Sci.*, 2003, **88**, 1032–1039.
25 Y. Chen, Q. Zhang, Q. Han, Y. Mi, S. Sun, C. Feng, H. Xiao, P. Yu and C. Yang, *J. Appl. Polym. Sci.*, 2017, **134**, 44721–44729.
26 H. Kocer, I. Cerkez, S. Worley, R. Broughton and T. Huang, *ACS Appl. Mater. Interfaces*, 2011, **3**, 3189–3194.
27 L. Bastarrachea and J. Goddard, *J. Agric. Food Chem.*, 2015, **63**, 4243–4251.
28 R. Padmanabhuni, J. Zengbing and Y. Sun, *Ind. Eng. Chem. Res.*, 2015, **51**, 5148–5156.
29 L. Bastarrachea and J. Goddard, *J. Appl. Polym. Sci.*, 2012, **127**, 821–831.
30 T. Ren, M. Qiao, L. Zhang, J. Weese, T. Huang and X. Ren, *J. Food Prot.*, 2018, **81**, 195–201.
31 M. Kazemian, L. Wang and S. Liu, *ACS Appl. Bio Mater.*, 2019, **2**, 5021–5031.
32 B. Demir, R. Broughton, T. Huang, M. Bozack and S. Worley, *Ind. Eng. Chem. Res.*, 2017, **56**, 11773–11781.
33 D. Chang, Z. li, X. Wang, C. Zhu, A. Dong and G. Gao, *Colloids Surf., B*, 2018, **163**, 402–411.
34 E. Kenawy, S. Worley and R. Broughton, *Biomacromolecules*, 2007, **8**, 1359–1384.
35 A. Dong, Y. Wang, Y. Gao, T. Gao and G. Gao, *Chem. Rev.*, 2017, **117**, 4806–4862.
36 F. Hui and C. Debiemme-Chouvy, *Biomacromolecules*, 2013, **14**, 585–601.
37 V. Ravichandran, R. Rai, V. Kesavan and A. Jayakrishnan, *J. Biomater. Sci., Polym. Ed.*, 2017, **28**, 2131–2142.
38 R. Rai and A. Jayakrishnan, *New J. Chem.*, 2018, **42**, 12152–12161.
39 R. Rai and A. Jayakrishnan, *New J. Chem.*, 2019, **43**, 3778–3787.
40 G. Sun and S. Worley, *J. Chem. Educ.*, 2005, **82**, 60.
41 M. Abdallah, M. Salem, B. Al Jahdaly, M. Awad, E. Helal and A. Fouda, *Int. J. Electrochem. Sci.*, 2017, **12**, 4543–4562.
42 X. Yanlong, Z. Lei, S. Yongfeng, L. Ning, L. Yongli, L. Bin, X. Qinghua, H. Chaoliang and C. Xuesi, *Chem. Res. Chin. Univ.*, 2015, **35**, 651–657.
43 F. Zhang, E. Kang, K. Neoh, P. Wang and K. Tan, *Biomaterials*, 2001, **22**, 1541–1548.
44 A. Cossu, Y. Si, G. Sun and N. Nitin, *Appl. Environ. Microbiol.*, 2017, 83.
45 V. Kapoor, R. Rai, D. Thiyagarajan, S. Mukherjee, G. Das and A. Ramesh, *ChemBioChem*, 2017, **18**, 1557.
46 M. Qiao, T. Ren, T. Huang, J. Weese, Y. Liu, X. Ren and R. Farag, *RSC Adv.*, 2017, **7**, 1233–1240.
47 M. Theiszova, S. Jantova, J. Dragunova, P. Grznarova and M. Palou, *Biomed. Pap. Med. Fac. Palacky Univ. Olomouc Czech. Repub.*, 2005, **149**, 393–396.
48 T. Ponrasu, P. Vishal, R. Kannan, L. Suguna and V. Muthuvijayan, *RSC Adv.*, 2016, **6**, 73617–73626.